Available online at www.sciencedirect.com
SCIENCE DIRECT®
Journal of Solid State Chemistry 177 (2004) 2329–2338
JOURNAL OF SOLID STATE CHEMISTRY
http://elsevier.com/locate/jssc

Controlled synthesis of single-crystalline $Mg(OH)_2$ nanotubes and nanorods via a solvothermal process

Weiliu Fan, Sixiu Sun,* Xinyu Song, Weimin Zhang, Haiyun Yu, Xuejie Tan, and Guangxiang Cao

Department of Chemistry, Shandong University, 27 Nanlu, Jinan Shandong Province 250100, PR China

Received 17 December 2003; received in revised form 17 March 2004; accepted 21 March 2004

Abstract

The synthesis of $Mg(OH)_2$ one-dimensional (1D) nanostructures was systematically investigated in different solvents at various temperatures with $Mg_{10}OH_{18}Cl_2 \cdot 5H_2O$ nanowires as source materials. The results showed that the characters of the products, such as crystal size, shape, and structure, were strongly influenced by the solvent and temperature during the solvothermal process. 1D nanotubes of $Mg(OH)_2$, with 80–300 nm outer diameter, 30–80 nm wall thickness, and several tens of micrometers in length were obtained by choosing bidentate ligand solvents such as ethylenediamine and 1,6-diaminohexane as the reaction solvent. But when using monodentate ligand pyridine as the reaction solvent, the obtained samples showed nanorods morphology. The $Mg(OH)_2$ thus produced was analyzed by X-ray powder diffraction (XRD), transmission electron microscopy (TEM), high-resolution electron microscopy (HRTEM), and selected-area electron diffraction (SAED). The possible growth mechanism of the 1D nanostructure $Mg(OH)_2$ was discussed.

Keywords: $Mg(OH)_2$; Nanotubes; Nanorods; Solvothermal

1. Introduction

Over the past decade, one-dimensional (1D) nano-sized building blocks such as nanorods, nanowires and nanotubes have attracted intense interest because of their distinctive geometries, novel physical and chemical properties, and potential applications in nanodevices [1,2]. These systems are of at least one restricted dimension, which could offer new opportunities for investigating their size- and shape-dependent optical, magnetic, and electronic properties [3–6].

The key to preparing a 1D nanostructure is the way in which atoms or other building blocks are rationally assembled into a structure with nanometer size but a much larger length [3b,7]. Generally, 1D nanostructures can be fabricated by template-directed growth methods [8–10], which include hard template (such as porous anodic aluminum and carbon nanotubes) and soft templates (such as liquids and polymers), the vapor–liquid–solid (VLS) mechanism [11], the vapor–solid (VS) mechanism [12], arc discharge [13] and laser ablation [3b]. All of these methods are very useful and of widespread importance, but there are some limitations to their utilities. For example, some methods suffer from the requirements of complicated apparatus, relatively elevated temperature, and others need special conditions, or tedious procedures. Solution approaches have also been explored for the synthesis of 1D nanostructures [5,14–19]. Previous work has shown that the solvothermal/hydrothermal process is a versatile route for the synthesis of various semiconductor nanorods [20,21], lanthanide hydroxide nanorods [22a], and thin Te nanobelts/tubes [22b].

Magnesium hydroxide ($Mg(OH)_2$) has been known for a long time and is used for medical and industrial products in broad fields. In recent research, it is found that $Mg(OH)_2$ can be used as starting product for controlling the synthesis of the nanoscale magnesium oxide (MgO), and the crystallite size, morphological features of $Mg(OH)_2$ can be retained well [23,24]. When MgO is prepared in the 1D form it can be expected to have many special properties, such as MgO nanorods are expected to have many novel mechanical, catalytic,

*Corresponding author. Fax: +865318564464.
E-mail address: ssx@sdu.edu.cn (S. Sun).

0022-4596/$ - see front matter © 2004 Elsevier Inc. All rights reserved.
doi:10.1016/j.jssc.2004.03.028

and electronic properties due to their extremely small size, large anisotropy, and perfect crystallinity. They could find many applications in functional composites as reinforcing agents and artificial pinning centers, as demonstrated in nanostructured high-temperature superconductors (HTSCs) [23], thus, preparing the 1D structure $Mg(OH)_2$ is important. But to the best of our knowledge, there are few reports on the synthesis of 1D nanostructure $Mg(OH)_2$, especially $Mg(OH)_2$ nanotubes. Li and co-workers have prepared $Mg(OH)_2$ nanorods by the solvothermal method; in the report, the obtained samples are mainly rodlike, however, mixed with small amounts of nanofibers and nanotubes [23].

Recently, we successfully synthesized tubelike $Mg(OH)_2$ nanocrystallines through a simple solvothermal technique [25]. Our previous studies have only focused on the formation of the nanotubes. Further investigations demonstrated that the crystallite shape and structure of the obtained products could be controlled well by this solvothermal method. In this communication, we present a controlled solvothermal route that has been developed in our synthesis of single-crystal $Mg(OH)_2$ nanotubes and nanorods, by the in situ disposition $Mg_{10}OH_{18}Cl_2 \cdot 5H_2O$ nanowires in a variety of solvents at a proper temperature and duration time. The yields of both nanotubes and nanorods are very high, whose morphology and structure appear to be distinctively different from the ones reported in the literature [23,24,26].

2. Experimental section

2.1. Materials

All chemicals used in this work, such as magnesium chloride ($MgCl_2 \cdot 6H_2O$), magnesium oxide (MgO), ethylenediamine, 1,6-diaminohexane, pyridine and aqueous ammonia ($NH_3 \cdot H_2O$, 25 wt%) were A.R. regents from the Tianjing Chemical Factory, China.

2.2. Synthesis of $Mg_{10}OH_{18}Cl_2 \cdot 5H_2O$ nanowires

The solid magnesium chloride hydroxide hydrate, which can also be called basic magnesium chloride, formed in the system $MgO–MgCl_2–H_2O$ is a components of Sorrel's cement. Previous papers have reported the study of the chemical reactions in the system $MgO–MgCl_2–H_2O$ [27,28]. The procedure that yields $Mg_{10}OH_{18}Cl_2 \cdot 5H_2O$ nanowires has been described in our previous work [25]. In a typical method, 200 mL of 3 mol/L magnesium chloride solution was placed in a constant-temperature bath at 70°C, and while the aqueous solution was stirred, an appropriate amount of magnesium oxide powder was slowly added to it. The mixture was fully stirred to dissolve the added magnesium oxide almost completely. Then the heating was stopped, and the solution was left to stand at room temperature for 2 days. A white precipitation was obtained, the precipitation was filtered off, washed with distilled water and absolute ethanol several times, respectively, and then dried in an oven at 50°C for 3 h to obtain the basic magnesium chloride nanowires in the form of $Mg_{10}OH_{18}Cl_2 \cdot 5H_2O$.

2.3. Controlled solvothermal synthesis of $Mg(OH)_2$ nanotubes and nanorods

Our solvothermal reaction to produce $Mg(OH)_2$ nanotubes is analogous to the reported method [23,24]. An appropriate amount of basic magnesium chloride ($Mg_{10}OH_{18}Cl_2 \cdot 5H_2O$) nanowires was added into a Teflon-lined autoclave of 50 mL capacity. Then the autoclave was filled with various organic solvents, such as ethylenediamine, 1,6-diaminohexane and pyridine up to 70% of the total volume. The autoclave was sealed into a stainless-steel tank and maintained at 70–180°C for 2–6 h without shaking and stirring. After cooling to room temperature naturally, the sample was filtered off, washed with distilled water and absolute ethanol, respectively, and then dried in a vacuum at 50°C for 3 h.

In contrast, the as-prepared basic magnesium chloride ($Mg_{10}OH_{18}Cl_2 \cdot 5H_2O$) nanowires were treated with a hydrothermal process using aqueous ammonium ($NH_3 \cdot H_2O$), distilled water (H_2O), ethanol (EtOH) and EtOH–H_2O (1:1, v/v) as solvent, respectively, under the same reaction conditions as the nonaqueous organic alkylamine solvothermal procedure.

2.4. Characterization of samples

The overall crystallinity and purity of the as-synthesized sample were examined by X-ray diffraction (XRD) using a Japan Rigaku D/Max-γA rotation anode X-ray diffractometer equipped with graphite monochromatized Cu$K\alpha$ radiation ($\lambda = 1.54178$ Å) at a scanning rate of $0.02^\circ\,s^{-1}$ in the 2θ range from 10° to 70°.

The morphologies and micro- and nanostructure of the as-synthesized magnesium hydroxide products were characterized by transmission electron microscopy (TEM) and electron diffraction (ED), carried out using JEOL 6300 at an accelerating voltage of 100 kV. The samples for these measurements were dispersed in absolute ethanol by vibration in the ultrasonic pool. Then, the solutions were dropped onto a copper grid coated with amorphous carbon films and dried in air before performance.

More details about the structure of the 1D nanotubes and nanorods were investigated by the selected area electron diffraction (SAED) pattern and high-resolution

transmission electron microscopy (HRTEM), using HITACHI 9000-NAR high-resolution transmission electron microscope (HRTEM) performed at 300 kV.

Infrared spectra of the samples were obtained on a Nicolet FT-IR5DX spectrometer.

3. Results

3.1. Formation of $Mg_{10}OH_{18}Cl_2 \cdot 5H_2O$ nanowires

Fig. 1a shows XRD spectra of the samples basic magnesium chloride; all the reflections can be indexed to monoclinic phase of $Mg_{10}OH_{18}Cl_2 \cdot 5H_2O$ (JCPDS 7-409). The low-magnification TEM image in Fig. 1b shows the as-prepared sample consisting entirely of very long wirelike nanostructures with diameters in the range of 100–300 nm and lengths of up to several hundreds of micrometers. At higher magnification (Fig. 1c) it can be verified that nanowires have a relatively uniform width and sharp boundary on this scale. Fig. 1d gives a typical electron diffraction (ED) pattern that was obtained by focusing the beam on an individual nanowire; it clearly shows that the nanowires are well crystallized.

3.2. Formation of $Mg(OH)_2$ 1D nanostructure

The solvothermal reaction to prepare $Mg(OH)_2$ 1D structure using $Mg_{10}OH_{18}Cl_2 \cdot 5H_2O$ nanowires as a precursor in a variety of solvents at a proper temperature and duration time yielded very interesting results. Solvent and reaction temperature played a crucial role in controlling the growth of crystallites. We made full use of these interesting results to develop the chemical control synthesis methods in crystal shape, size, and structure.

In the whole solvothermal reaction process, to understand the possible mechanism of the formation of $Mg(OH)_2$ 1D structure, controlled experiments under different conditions were conducted. The detailed conditions and the results of the experiments are listed in Table 1, and all the products are characterized by XRD and TEM.

3.2.1. Formation of $Mg(OH)_2$ nanotubes with ethylenediamine as the reaction solvent

First, a series of solvothermal synthetic experiments with $Mg_{10}OH_{18}Cl_2 \cdot 5H_2O$ precursors in ethylenediamine solvent were carried out in various reaction temperatures and duration times (Table 1, experiments 1–6). Fig. 2 shows the XRD patterns of the products.

Figs. 2a–d are the patterns of the products obtained from the solvothermal treatments of the $Mg_{10}OH_{18}Cl_2 \cdot 5H_2O$ precursors at 70°C, 120°C, 150°C, 180°C for 6 h, respectively. We can see from these patterns that when the reaction temperature is below 70°C, the products exhibit a hexagonal phase of $Mg(OH)_2$ (JCPDS file No. 7-239), but the peaks at about 12.9°, 21.9°, 26.1°, and 49.6° (marked with ■ in the pattern) cannot be indexed to any known phase of $Mg(OH)_2$ or $Mg_{10}OH_{18}Cl_2 \cdot 5H_2O$ in the standard JCPDS cards. It have resulted from the complex formed by ethylenediamine with the $Mg_{10}OH_{18}Cl_2 \cdot 5H_2O$ precursor, which will be discussed in the following reaction mechanism sections. As the reaction temperature rises to over 120°C pure hexagonal $Mg(OH)_2$ is the only product, no characteristic peaks from other crystalline forms are detected in the XRD pattern that the peak of the imagined complex disappears, and we can see from

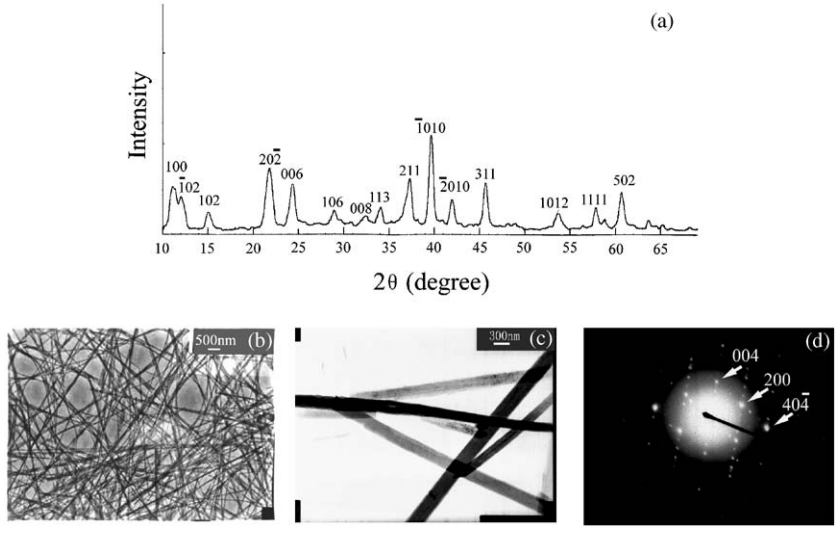

Fig. 1. (a) XRD pattern of as-prepared basic magnesium chloride; (b) and (c) Typical TEM images of $Mg_{10}OH_{18}Cl_2 \cdot 5H_2O$ nanowires, (d) a typical ED pattern that was obtained by focusing the beam on an individual nanowire.

Table 1
Experimental conditions and results of the experiments

Sample no.	Solvent	Temperature (°C)	Duration time (h)	Products phase	Morphology
1	Ethylenediamine	70	6	$Mg(OH)_2$ hexa. with some other complexes	Tubelike + rodlike
2	Ethylenediamine	120	6	$Mg(OH)_2$ hexa.	Tubelike
3	Ethylenediamine	150	6	$Mg(OH)_2$ hexa.	Tubelike
4	Ethylenediamine	180	6	$Mg(OH)_2$ hexa.	Tubelike
5	Ethylenediamine	180	4	$Mg(OH)_2$ hexa.	Tubelike
6	Ethylenediamine	180	2	$Mg(OH)_2$ hexa.	Tubelike
7	1.6-diaminohexane	180	6	$Mg(OH)_2$ hexa.	Tubelike
8	Pyridine	180	6	$Mg(OH)_2$ hexa.	Rodlike
9	$NH_3 \cdot H_2O$	180	6	$Mg(OH)_2$ hexa.	Irregular particles
10	H_2O	180	6	$Mg(OH)_2$ hexa.	Platelike
11	EtOH–H_2O (1:1)	180	6	$Mg(OH)_2$ hexa.	Platelike
12	EtOH	180	6	$Mg(OH)_2$ hexa.	Platelike

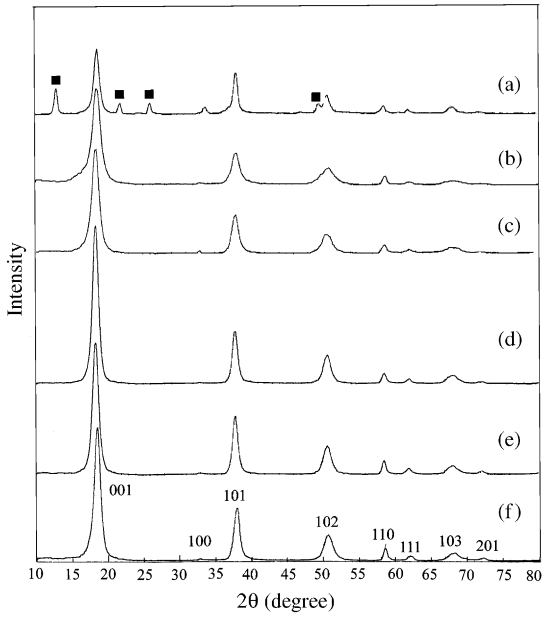

Fig. 2. XRD patterns of the products prepared using ethylenediamine as reaction solvent at (a) 70°C for 6 h (■, the phase maybe of the complex formed by ethylenediamine with $Mg_{10}OH_{18}Cl_2 \cdot 5H_2O$); (b) 120°C for 6 h; (c) 150°C for 6 h; (d) 180°C for 6 h; (e) 180°C for 4 h; (f) 180°C for 2 h.

the XRD pattern, with the increase of the reaction temperature, the relative intensities of the diffraction peaks increase, i.e. a higher temperature will generate higher crystallinity.

Figs. 2d–f show the patterns of the products prepared from the ethylenediamine solvothermal treatments of the precursors for 6, 4, 2 h, respectively, with the reaction temperature kept constant at 180°C, we can see no significant differences in these patterns. In addition, from the patterns we can also see that the relative intensities of each peak is not too consistent with the JCPDS standard card file (No. 7-239), where 101 is the strongest lattice plane and 0 0 1 ranks second. Here, we observe converse intensities for these two lattice planes, which indicates that preferred orientations might occur along (001) or some other lattice planes [29]. The signification variation of intensity between 0 0 1 and other lattice planes implies an unusual shape of the products. This agrees well with the TEM results as will be described below. We believe that the abundance of (001) planes in the anisotropic shape of the 1D nanostructure results in the remarkable increase in the intensity of the 0 0 1 reflection [21,30].

IR absorbance measurements (Fig. 3) of the as-synthesized products and their starting material $Mg_{10}OH_{18}Cl_2 \cdot 5H_2O$ also provide interesting results. The IR spectra of the products prepared by the solvothermal treatments of the $Mg_{10}OH_{18}Cl_2 \cdot 5H_2O$ precursors at 70°C for 6 h (Fig. 3c) exhibit vibration peaks corresponding to $Mg_{10}OH_{18}Cl_2 \cdot 5H_2O$ (Fig. 3b). Different from pure $Mg_{10}OH_{18}Cl_2 \cdot 5H_2O$, it is more complicated, the N–H twisting and rocking vibrations at frequencies about 1580 and 900–650 cm^{-1} and the C–H wagging and scissoring vibrations at frequencies about 1470 and 1380 cm^{-1} can be found. But these vibrations exhibit many differences from the pure ethylenediamine (Fig. 3a), which could be due to the ordered alignment and regular conformation of ethylenediamine molecules in the products, while in liquid-state ethylenediamine the orientation and conformation of the molecules are randomized due to thermal perturbation. When the reaction temperature increased above 120°C, the IR spectra of the products exhibited typical vibrations of $Mg(OH)_2$ as shown in Figs. 3d–f. So the IR spectra give information on the reaction mechanism, and the result is well consistent with the results of the XRD characterization.

TEM investigations show that the reaction products resulting from the solvothermal treatment with ethylenediamine as a solvent at 70°C, 120°C, 150°C, and 180°C for 6 h, respectively, consist exclusively of isolated and starlike grown-together nanotubes (Fig. 4). The

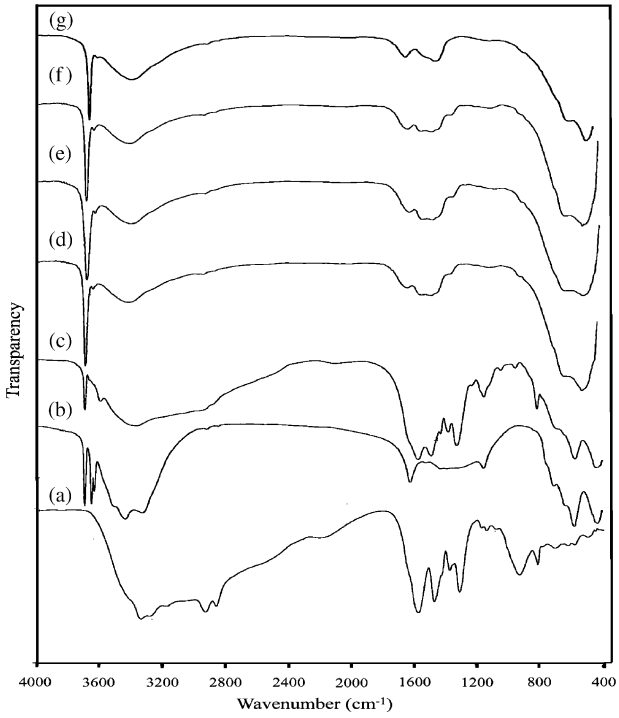

Fig. 3. FTIR spectrum of ethylenediamine (a) and the as-synthesized $Mg_{10}OH_{18}Cl_2 \cdot 5H_2O$ (b); (c), (d), (e), and (f) is the FTIR spectrum of the products obtained from solvothermal treatment of the $Mg_{10}OH_{18}Cl_2 \cdot 5H_2O$ nanowires in ethylenediamine at 70°C, 120°C, 150°C, 180°C for 6 h, respectively; the spectrum of pure phase $Mg(OH)_2$ is shown in (g).

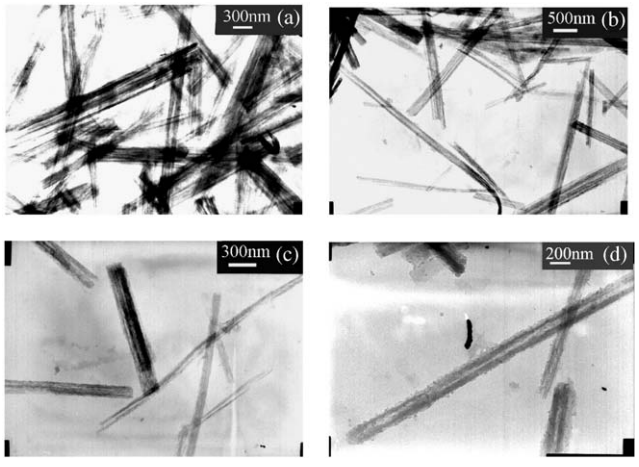

Fig. 4. TEM images of the products prepared with ethylenediamine as reaction solvent at (a) 70°C for 6 h; (b) 120°C for 6 h; (c) 150°C for 6 h; and (d) 180°C for 6 h.

resultant products initially appeared in the form of nanotube bundles and solid nanorods, as shown in Fig. 4a. When the reaction temperature was elevated to 120°C, and 150°C, respectively, the crystallinity of the as-obtained samples obviously improved, and some isolated nanotubes were observed, as shown in

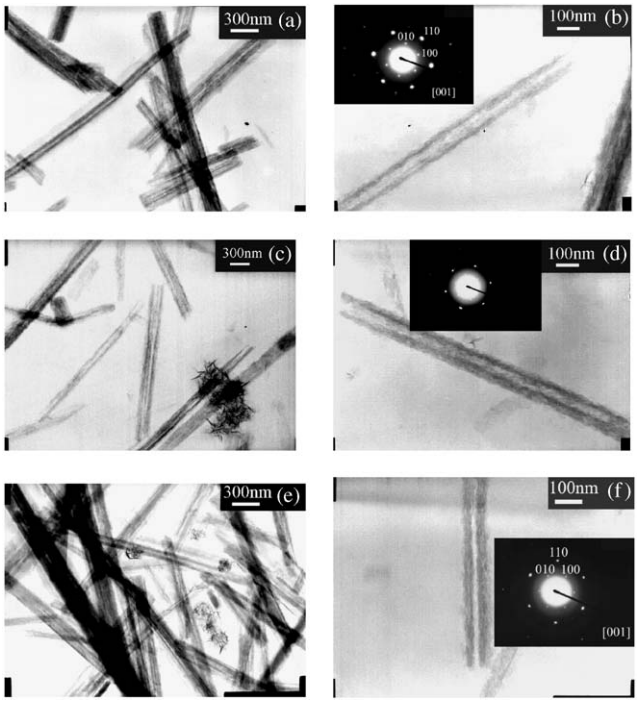

Fig. 5. TEM images and ED patterns of the obtained samples by solvothermal disposing $Mg_{10}OH_{18}Cl_2 \cdot 5H_2O$ nanowires with ethylenediamine as a reaction solvent at (a and b) 180°C for 2 h; (c and d) 180°C for 4 h; (e and f) 180°C for 6 h. The ED patterns inset in (b, d, and f) indicates the single-crystalline nature of the sample, and its hexagonal phase, as it well consistent with the XRD characterization.

Figs. 4b and c. After the temperature was elevated to 180°C, the crystallinity was higher than that of the former. The clear contrast (the outer part is darker than the inner part of the 1D structure) suggests that the nanotube is well crystallized. It could be seen from the TEM images that the variation in the morphologies of the products with different reaction temperatures is significant, and in this case, a higher solvothermal temperature is used to improve the crystallinity and the purity of the products, which is well consistent with the XRD analysis, and which might provide some clues to understand the growth process.

To investigate the details of the solvothermal process, different solvothermal periods were employed to investigate the influence of the reaction time on the morphologies of the products with the reaction temperature fixed at 180°C. Fig. 5 shows TEM images of the $Mg(OH)_2$ products resulting from the solvothermal treatment of the $Mg_{10}OH_{18}Cl_2 \cdot 5H_2O$ nanowires precursors for 2, 4, and 6 h, respectively. Figs. 5a, c and e give typical whole images of the $Mg(OH)_2$ products; from these images one can see that the as-synthesized samples consist almost entirely of nanotubes, and no significant variation of the morphologies can be found; the nanotubes have outer diameters of 80–300 nm, wall thickness of 30–80 nm, and lengths of several tens of

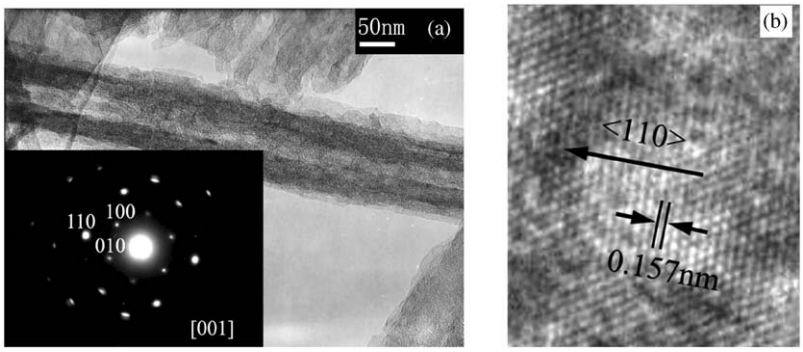

Fig. 6. (a) The TEM image and SAED pattern (inset) of a $Mg(OH)_2$ nanotube prepared by ethylenediamine solvothermal disposing $Mg_{10}OH_{18}Cl_2 \cdot 5H_2O$ nanowires at 180°C for 6 h. The diffraction spots could be indexed to the hexagonal structure; this assignment is further supported by the HRTEM image shown in (b). The longitudinal axis of such nanotubes of hexagonal $Mg(OH)_2$ was along the [110] direction. The fringe spacing ($\sim$0.157 nm) observed in this image acquired from the region indicated by the rectangle corresponds to the separation between the (110) lattice planes. The HRTEM image was taken on a HITACHI 9000-NAR-transmission electron microscope.

micrometers. Figs. 5b, d and f show that a well-crystallized single nanotube of the sample corresponds to Figs. 5a, c and e with reaction times for 2, 4, and 6 h, respectively. From the images, one can see that the nanotubes have open ends and a straight cylindrical morphology. Each nanotube has a uniform outer (inner) diameter and wall thickness. The highly crystalline nature of our $Mg(OH)_2$ nanotubes was further confirmed by electron diffraction. The ED patterns' inset in Figs. 5b, d and f show discrete spots, indicating the single-crystalline nature of the sample, and its hexagonal phase, which is well consistent with the results of the XRD characterization (Figs. 2d, e and f). On the other hand, the relative yield of $Mg(OH)_2$ nanotubes monitored by TEM increased with the reaction time, this is to say, reaction time affects merely the overall yield of the nanotube, instead of the morphology.

The crystallinity of the tubular structure was further examined with high-resolution TEM (HRTEM) and selected-area electron diffraction (SAED). Fig. 6a shows the low-magnification TEM image of a typical $Mg(OH)_2$ nanotube with the outer diameter ca. 100 nm. The SAED pattern inset recorded perpendicular to the growth axis of the single nanotube could be attributed to the [001] zone axis diffraction of hexagonal phase $Mg(OH)_2$, and this suggested that the nanotube grew along the [110] direction. Diffraction patterns taken from different regions of this individual nanotube were essentially the same; such homogeneity in crystalline structure and orientation along each nanotube implies that the $Mg(OH)_2$ nanotubes synthesized using the present procedure were well crystallized in structure. These conclusions were also confirmed by HRTEM studies (see Fig. 6b), and the regular fringe spacing of 0.157 nm calculated from this image agreed well with the expected separation between the (110) lattice planes.

Based on the XRD, TEM, HRTEM, and SAED analysis of the obtained $Mg(OH)_2$ products from experiments 1–6, we can conclude that the optimal conditions for the growth of well-developed tubular crystals are when the temperature is at 180°C, and the reaction time is more than 2 h.

3.2.2. Formation of $Mg(OH)_2$ 1D nanostructures in 1,6-diaminohexane and pyridine

It is well known that solvent plays an important role in determining the crystal morphology. Solvents with different physical and chemical properties can influence the solubility, reactivity, and diffusion behavior of the reactants; in particular, the polarity and coordinating ability of the solvents can influence the crystal morphology of the final product. We substituted ethylenediamine with 1,6-diaminohexane and pyridine as a solvent kept the other reaction conditions constant (Table 1, experiments 7, 8), and found that in 1,6-diaminohexane the obtained $Mg(OH)_2$ was also in nanotube form, but in pyridine the obtained samples showed rodlike morphology.

The XRD patterns of the as-prepared samples using 1,6-diaminohexane and pyridine as the reaction solvent, respectively, are shown in Figs. 7a and b, respectively. All diffraction peaks can also be indexed as hexagonal phase magnesium hydroxide with calculated lattice parameters comparable to that of JCPDS standard card (No. 7-239). No XRD peaks arising from impurities can be detected. From the patterns we can also see that the relative intensities of each peak are not too consistent with the JCPDS standard card file (No. 7-239), which is similar to the patterns resulting from the ethylenediamine solvothermal procedure.

Figs. 8a and b illustrate the typical TEM image of $Mg(OH)_2$ nanotubes obtained from solvothermal treatment of the $Mg_{10}OH_{18}Cl_2 \cdot 5H_2O$ nanowires in

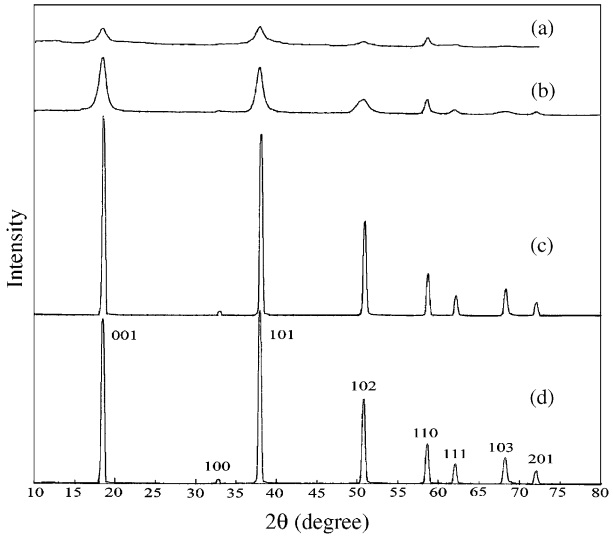

Fig. 7. XRD patterns of obtained samples by solvothermal/hydrothermal disposing $Mg_{10}OH_{18}Cl_2 \cdot 5H_2O$ nanowires (a) in 1,6-diaminohexane at 180°C for 6 h; (b) in pyridine at 180°C for 6 h; (c) in aqueous ammonium at 180°C for 6 h; (d) in distilled water at 180°C for 6 h.

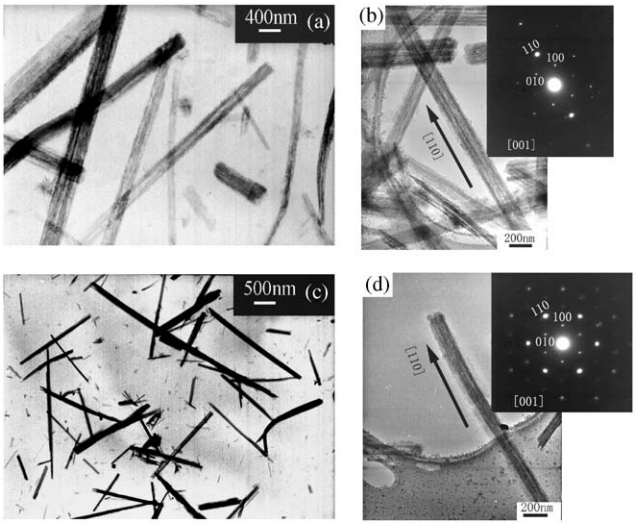

Fig. 8. (a) Typical TEM image of $Mg(OH)_2$ nanotubes obtained from solvothermal treatment of the $Mg_{10}OH_{18}Cl_2 \cdot 5H_2O$ nanowires in 1,6-diaminohexane at 180°C for 6 h; (b) The TEM image and SAED pattern (inset) of a single $Mg(OH)_2$ nanotube; (c) Typical TEM image of $Mg(OH)_2$ nanorods prepared in pyridine at 180°C for 6 h; (d) The TEM image and SAED pattern (inset) of a $Mg(OH)_2$ nanorod. The diffraction spots could be indexed to the hexagonal structure.

1,6-diaminohexane at 180°C for 6 h. As can be seen the products consist of hollow tubelike morphology with outer diameters of 100–400 nm, wall thicknesses of 60–100 nm, and lengths of several tens of micrometers. Figs. 8c and d show TEM images of the $Mg(OH)_2$ products resulting from the solvothermal treatment of the $Mg_{10}OH_{18}Cl_2 \cdot 5H_2O$ nanowires precursors in pyridine at 180°C for 6 h, which comprises a rodlike

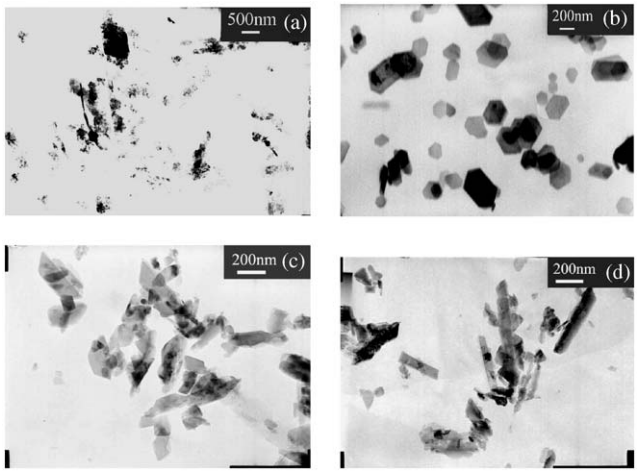

Fig. 9. TEM images of the products prepared in (a) in aqueous ammonium ($NH_3 \cdot H_2O$, 25 wt%) at 180°C for 6 h; (b) in distilled water (H_2O) at 180°C for 6 h; (c) in EtOH–H_2O (1:1, v/v)) at 180°C for 6 h; (d) in ethanol (EtOH) at 180°C for 6 h.

structure with average diameters of 200 nm and lengths of up to several micrometers. The SAED patterns (inset in Figs. 8b and d) recorded with the incident electron beam perpendicular to the growth axis of the 1D nanostructures can be indexed to the [001] zone axis diffraction of hexagonal phase $Mg(OH)_2$, and which revealed that the as-synthesized $Mg(OH)_2$ nanotubes and nanorods are structurally uniform, with a growth direction of [110]. This result is well consistent with that of the nanotubes prepared in ethylenediamine.

3.2.3. *Comparative experiments with distilled water and ammonia as the reaction solvent*

To explore the key factor of the chemical control synthesis process, we also chose aqueous ammonium ($NH_3 \cdot H_2O$), distilled water (H_2O), ethanol (EtOH) and EtOH–H_2O (1:1, v/v), respectively, as the reaction solvent for the comparative experiments (Table 1 experiments 9–12).

The phase composition and phase structure of the as-synthesized products were examined by XRD. Fig. 7c shows the pattern of the sample produced in aqueous ammonium. All the reflections can be indexed to be a pure hexagonal phase of $Mg(OH)_2$ (JCPDS No. 7-239). Compared with the XRD patterns of the samples produced in nonaqueous alkylamine solvents, all the peaks are sharp and strong. There is a bit stronger (001) peak in the pattern than expected, but the TEM image (Fig. 9a) shows that $Mg(OH)_2$ crystal growth in aqueous ammonium was not oriented. The morphology of the $Mg(OH)_2$ crystallites are irregular nanocrystals and the average particle size is about 200 nm.

Fig. 7d shows the pattern of the sample obtained in distilled water. All the strong and sharp reflection peaks of the pattern can be indexed to the hexagonal phase of

$Mg(OH)_2$, with lattice parameters $a = 3.147$ Å and $c = 4.770$ Å comparable to that of JCPDS standard card (No. 7-239). No XRD peaks arising from impurities can be detected and no variation of intensity between (001) and other lattice planes can be found. The TEM image (Fig. 9b) shows that the morphology of the $Mg(OH)_2$ crystallites as-obtained in distilled water solvent is hexagonal plateletlike particles, with diameter ranging from 0.2 to 0.6 μm.

Figs. 9c and d display TEM images of $Mg(OH)_2$ particles obtained in EtOH–H_2O (1:1, v/v)) and ethanol, respectively (XRD patterns are not given). The $Mg(OH)_2$ particles synthesized in EtOH–H_2O (1:1, v/v)) comprise plate particles with diameter 100–200 nm. The TEM image in Fig. 9d demonstrates that the $Mg(OH)_2$ obtained in ethanol comprises short nanorods with diameter 80–100 nm, length 150–500 nm. Compared with distilled water as solvent, it seems the aspect ratio becomes larger. The results demonstrate that the polarity of the solvent has some effects on the morphology of nanocrystalline $Mg(OH)_2$.

4. Discussion

We now come back to discuss the growth mechanism of the $Mg(OH)_2$ 1D nanostructures (nanotubes and nanorods). In this work, we have studied the effect of media on the synthesis of $Mg(OH)_2$, in order to optimize the experimental conditions. Although all the selected solvents provide a conducive conduction for $Mg(OH)_2$ formation, they have different influences. The variation of crystal morphology in the different media is an important experimental phenomenon. To our knowledge, the chemical and physical mechanisms still remain elusive, even though many researchers have attributed this variation to many factors [29]. In our process, factors such as the nature of the crystal structure, the coordination chemistry, reaction temperature and heating time might be involved.

During the experiment, we find that the starting material $Mg_{10}OH_{18}Cl_2 \cdot 5H_2O$ nanowires are not stable in solvent (such as aqueous ammonium ($NH_3 \cdot H_2O$), distilled water (H_2O), ethanol (EtOH) and EtOH–H_2O (1:1, v/v)) under the heating conditions; the Cl^- can be exchanged by the OH^-, so it is easy to lose the fibrous morphology to convert into $Mg(OH)_2$ particles as shown in Fig. 9. By the above analysis, we find that choosing an appropriate ligand that has one anchor atom in it is necessary and sufficient for the transformation from $Mg_{10}OH_{18}Cl_2 \cdot 5H_2O$ nanowires to $Mg(OH)_2$ 1D nanostructures. Alkylamine was selected as the solvent due to its special properties, such as basic capacity, strong chelation, and its ability to act as an absorber of the excess heat released in the reaction.

Ethylenediamine is an excellent template for the formation of 1D materials, because of the N-chelation and its structure [31,32]. The role of ethylenediamine as a structure-directing coordination molecular template (SCMT) responsible for the morphologies of the $Mg(OH)_2$ products has been discussed in our previous report [25]; that work provided further insights into the SCMT mechanism previously proposed by Li and coworkers to explain the growth mechanism of CdE (E = S, Se, Te) nanorods in ethylenediamine [33]. In a typical SCMT process, ethylenediamine acts as a template molecule, which is incorporated into the inorganic framework first and then escapes from it to form nanocrystallites with desired morphologies.

In our process, during the solvothermal treatments of the starting material ($Mg_{10}OH_{18}Cl_2 \cdot 5H_2O$ nanowires), the organic alkylamine solvent may act as an N-chelating donor ligand to form a relatively stable complex with Mg^{2+} of the starting material ($Mg_{10}OH_{18}Cl_2 \cdot 5H_2O$), which is proved by the XRD pattern (Fig. 2a); the complex retains the 1D nanostructure morphology. During solvothermal process, the stability of the complex is expected to decrease with increasing temperature. At some relatively high temperature, the hydroxyl groups (OH) supplied by the crystal water may coordinate with the above complex and the Cl may be gradually lost; the reaction is essentially a substitution reaction. As the OH attacks the complex, which causes the bonds between Mg^{2+} and the N atoms of ethylenediamine to become weaker, finally Mg^{2+} and the N atoms separate from each other. Mg^{2+} is connected by OH and in the end they form a 1D $Mg(OH)_2$ nanostructure (nanotubes and nanorods), such as reported in the literature [22], and we found that nanotubes are always obtained by choosing bidentate ligand solvents such as ethylenediamine and 1,6-diaminohexane as the reaction solvent, but when using pyridine as the reaction solvent, the obtained samples show nanorods morphology.

But why the 1D nanostructures display different morphologies, i.e. hollow nanotube and solid nanorod, in different organic alkylamine solvents still remains obscure. It may be produced due to two factors. First, the coordination chemistry of the alkylamine solvents may have important effects on the formation of the 1D nanostructure. Ethylenediamine and 1,6-diaminohexane are bidentate ligands, during the reaction they probably use the *trans* conformation to bridge adjacent Mg^{2+} on the surface of $Mg_{10}OH_{18}Cl_2 \cdot 5H_2O$ [20c,21]; while the pyridine molecule has only one anchor atom, its coordination mode with metal ions must be monodentate. Then the different coordinating conformation mode results in the different morphologies in the solvothermal procedure. Second, from the structural point of view, the precursor $Mg_{10}OH_{18}Cl_2 \cdot 5H_2O$ has a monoclinic structure, and $Mg(OH)_2$ has a hexagonal

structure; both are incompatible in structure. Thus, the formation of 1D nanostructures (nanotubes and nanorods) may be possible in the organic alkylamine solvents.

5. Conclusions

We demonstrated in a previous work that single-crystal $Mg(OH)_2$ nanotubes with the growth direction along the [110] can be synthesized through a solution-based chemical route under controlled solvothermal conditions, using ethylenediamine as a reaction solvent, and the $Mg_{10}OH_{18}Cl_2 \cdot 5H_2O$ nanowires as precursors without the presence of any catalysts or templates. To explore the reaction mechanism, different synthetic reaction systems such as synthetic temperatures duration times and various solvents were investigated in this paper. The study showed that reaction temperature and the coordination ability of the selected solvent have important effects on the structure of the obtained samples. $Mg(OH)_2$ nanotubes 80–300 nm in outer diameter, 30–80 nm in wall thickness, and several tens of micrometers in length were obtained by choosing bidentate ligand solvents such as ethylenediamine and 1,6-diaminohexane as the reaction solvent. But when using monodentate ligand pyridine as the reaction solvent, the obtained samples showed solid nanorods morphology. The results further supported the proposed solvent coordination molecular template (SCMT) mechanism. Additionally, the present study has enlarged the family of nanotubes, and offers a possible solution-phase route to 1D single-crystal nanotubes and nanorods of other materials.

References

[1] (a) A.P. Alivisatos, Science 271 (1996) 933;
(b) H. Weller, Angew. Chem. Int. Ed. Engl. 32 (1993) 41;
(c) G.R. Patzke, F. Krumeich, R. Nesper, Angew. Chem. Int. Ed. 41 (2002) 2446.

[2] (a) X. Duan, Y. Huang, Y. Cui, J. Wang, C.M. Lieber, Nature 409 (2001) 66;
(b) N.I. Kovtyukhova, T.E. Mallouk, Chem. Eur. J. 8 (2002) 4355;
(c) S.H. Yu, B. Liu, M.S. Mo, J.H. Huang, X.M. Liu, Y.T. Qian, Adv. Funct. Mater. 13 (2003) 639.

[3] (a) C.M. Lieber, Solid State Commun. 107 (1998) 607;
(b) J.T. Hu, T.W. Odom, C.M. Lieber, Acc. Chem. Res. 32 (1999) 435.

[4] J.S. Bradley, B. Tesche, W. Busser, M. Masse, M.T. Reetz, J. Am. Chem. Soc. 122 (2000) 4631.

[5] (a) X.D. Peng, L. Manna, W.D. Yang, J. Wickham, E. Scher, A. Kadavanich, A.P. Alivisatos, Nature 404 (2000) 59;
(b) Z.A. Peng, X.G. Peng, J. Am. Chem. Soc. 123 (2001) 1389;
(c) Z.A. Peng, X.G. Peng, J. Am. Chem. Soc. 124 (2002) 3343.

[6] Y. Cui, Q.Q. Wei, H.K. Park, C.M. Lieber, Science 293 (2001) 1289.

[7] M.S. Mo, J.H. Zeng, X.M. Liu, W.C. Yu, S.Y. Zhand, Y.T. Qian, Adv. Mater. 14 (2002) 1658.

[8] (a) M.S. Sander, A.L. Prieto, R. Gronsky, T. Sands, A.M. Stacy, Adv. Mater. 14 (2002) 665;
(b) C.C. Tang, Y. Bando, T. Sato, K. Kurashima, Adv. Mater. 14 (2002) 1046.

[9] (a) H.J. Dai, E.W. Wong, Y.Z. Lu, S.S. Fan, C.M. Lieber, Nature 375 (1995) 769;
(b) W.Q. Han, S.S. Fan, Q.Q. Li, Y.D. Hu, Science 277 (1997) 1287.

[10] (a) J.H. Song, Y.Y. Wu, B. Messer, H. Kind, P.D. Yang, J. Am. Chem. Soc. 123 (2001) 10397;
(b) Y.D. Li, X.L. Li, R.R. He, J. Zhu, Z.X. Deng, J. Am. Chem. Soc. 124 (2002) 1411;
(c) E.D. Sone, E.R. Zubarev, S.I. Stupp, Angew. Chem. Int. Ed. 41 (2002) 1706.

[11] (a) A.M. Morales, C.M. Lieber, Science 279 (1998) 208;
(b) M. Huang, S. Mao, H. Feick, H. Yan, Y. Wu, H. Kind, E. Weber, R. Russo, P. Yang, Science 292 (2001) 189;
(c) X.F. Duan, C.M. Lieber, Adv. Mater. 12 (2000) 298.

[12] (a) Z.W. Pan, Z.R. Dai, Z.L. Wang, Science 291 (2001) 1947;
(b) Z.R. Dai, Z.W. Pan, Z.L. Wang, J. Am. Chem. Soc. 124 (2002) 8673;
(c) J.Y. Lao, J.G. Wen, Z.F. Ren, Nano Lett. 2 (2002) 1287;
(d) P. Yang, C.M. Lieber, Science 273 (1996) 4836.

[13] S. Iijima, Nature 354 (1991) 56.

[14] (a) T.J. Trentler, K.M. Hickman, S.C. Goel, A.M. Viano, P.C. Gibbons, W.E. Buhro, Science 270 (1995) 1791;
(b) W.E. Buhro, K.M. Hickman, T.J. Trentler, Adv. Mater. 8 (1996) 685.

[15] J.D. Holmes, K.P. Johnston, R.C. Doty, B.A. Korgel, Science 287 (2000) 1471.

[16] (a) M. Li, H. Schnableggar, S. Mann, Nature 402 (1999) 393;
(b) N.R. Jana, L. Gearheart, C.J. Murpyy, Adv. Mater. 13 (2001) 1389;
(c) S. Kwan, F. Kim, J. Akana, P. Yang, Chem. Commun. (2001) 447.

[17] S.H. Yu, M. Antonietti, H. Cölfen, M. Giersig, Angew. Chem. Int. Ed. 41 (2002) 2356.

[18] C. Pacholski, A. Kornowski, H. Weller, Angew. Chem. Int. Ed. 41 (2002) 1188.

[19] Z.Y. Tang, N.A. Kotov, M. Giersig, Science 297 (2002) 237.

[20] (a) S.H. Yu, Y.S. Wu, J. Yang, Z.H. Han, Y. Xie, Y.T. Qian, X.M. Liu, Chem. Mater. 10 (1998) 2309;
(b) S.H. Yu, J. Yang, Z.H. Han, Y. Zhou, R.Y. Yang, Y. Xie, Y.T. Qian, Y.H. Zhang, J. Mater. Chem. 9 (1999) 1283;
(c) J. Yang, J.H. Zeng, S.H. Yu, L. Yang, Y.H. Zhang, Y.T. Qian, Chem. Mater. 12 (2000) 3259;
(d) S.H. Yu, J. Yang, Y.S. Wu, Z.H. Han, Y. Xie, Y.T. Qian, Mater. Res. Bull. 33 (1998) 1661.

[21] J. Yang, C. Xue, S.H. Yu, J.H. Zeng, Y.T. Qian, Angew. Chem. Int. Ed. 41 (2002) 4697.

[22] (a) X. Wang, Y.D. Li, Angew. Chem. Int. Ed. 41 (2002) 4790;
(b) M. Mo, J. Zeng, X. Liu, W. Yu, S. Zhang, Y. Qian, Adv. Mater. 14 (2002) 1658.

[23] Y.D. Li, M. Sui, Y. Ding, G.H. Zhang, J. Zhuang, C. Wang, Adv. Mater. 12 (2000) 818.

[24] Y. Ding, G.T. Zhang, H. Wu, B. Hai, L.B. Wang, Y.T. Qian, Chem. Mater. 13 (2001) 435.

[25] W.L. Fan, S.X. Sun, L.P. You, G.x. Cao, X.Y. Song, W.M. Zhang, H.Y. Yu, J. Mater. Chem. 13 (2003) 3062.

[26] L. Yan, J. Zhuang, X.M. Sun, Z.X. Deng, Y.D. Li, Mater. Chem. Phys. 76 (2002) 119.

[27] A. Nørlund Christensen, P. Norby, J.C. Hanson, Acta Chem. Scand. 49 (1995) 331.

[28] A. Nørlund Christensen, P. Norby, J.C. Hanson, J. Solid State Chem. 114 (1995) 556.
[29] C. Wang, Y.D. Li, G.H. Zhang, J. Zhuang, G.Q. Shen, Inorg. Chem. 39 (2000) 4237.
[30] C.B. Murray, D.J. Norris, M.G. Bawendi, J. Am. Chem. Soc. 115 (1993) 8706.
[31] W.Z. Wang, Y. Geng, Y.T. Qian, M.R. Ji, X.M. Liu, Adv. Mater. 10 (1998) 1479.
[32] Y.D. Li, H.W. Liao, Y. Ding, Y.T. Qian, L. Yang, G.E. Zhou, Chem. Mater. 10 (1998) 2301.
[33] Y.D. Li, H.W. Liao, Y. Ding, Y. Fan, Y. Zhang, Y.T. Qian, Inorg. Chem. 38 (1999) 1382.